



Tumor immune microenvironment analysis of non-small cell lung cancer development through multiplex immunofluorescence

Jiaping Zhao^{1#}, Yu Lu^{1#}, Zhaofeng Wang^{2#}, Haiying Wang³, Ding Zhang⁴, Jinping Cai⁴, Bei Zhang⁴, Junling Zhang⁴, Mengli Huang⁴, Andreas Pircher⁵, Krishna H. Patel⁶, Honggang Ke¹, Yong Song²

¹Department of Thoracic Surgery, Affiliated Hospital of Nantong University, Medical School of Nantong University, Nantong, China; ²Department of Respiratory Medicine, Jinling Hospital, Affiliated Hospital of Medical School, Nanjing University, Nanjing, China; ³Department of Respiratory, Affiliated Hospital of Nantong University, Medical School of Nantong University, Nantong, China; ⁴Medical Affairs, 3D Medicines, Inc., Shanghai, China; ⁵Department of Haematology and Oncology, Internal Medicine V, Comprehensive Cancer Center Innsbruck (CCCI), Medical University of Innsbruck (MUI), Innsbruck, Austria; ⁶Institute for Translational Epidemiology, Icahn School of Medicine at Mount Sinai, New York, NY, USA

Contributions: (I) Conception and design: J Zhao, Y Lu, Z Wang, D Zhang; (II) Administrative support: H Ke, Y Song; (III) Provision of study materials or patients: J Zhao, Y Lu, Z Wang, H Wang; (IV) Collection and assembly of data: H Wang, D Zhang; (V) Data analysis and interpretation: B Zhang, J Zhang, M Huang; (VI) Manuscript writing: All authors; (VII) Final approval of manuscript: All authors.

[#]These authors contributed equally to this work.

Correspondence to: Honggang Ke, MD. Department of Thoracic Surgery, Affiliated Hospital of Nantong University, Medical School of Nantong University, No. 20 Xisi Road, Nantong 226001, China. Email: 601973500@qq.com; Yong Song, MD. Department of Respiratory Medicine, Jinling Hospital, Affiliated Hospital of Medical School, Nanjing University, No. 305 Zhongshan East Road, Nanjing 210002, China. Email: yong.song@nju.edu.cn.

Background: Emerging evidence has underscored the crucial role of infiltrating immune cells in the tumor immune microenvironment (TIME) of non-small cell lung cancer (NSCLC) development and progression. With the implementation of screening programs, the incidence of early-stage NSCLC is rising. However, the high risk of recurrence and poor survival rates associated with this disease necessitate a deeper understanding of the TIME and its relationship with driver alterations. The aim of this study was to provide an in-depth analysis of immune changes in early-stage NSCLC, highlighting the significant transitions in immune response during disease progression.

Methods: Tumor tissues were collected from 105 patients with precancerous lesions or stage I–III NSCLC. Next-generation sequencing (NGS) was used to detect cancer driver alterations. Multiplex immunofluorescence (mIF) was performed to evaluate immune cell density, percentage, and spatial proximity to cancer cells in the TIME. Next Among these patients, 64 had NGS results, including three with adenocarcinoma in situ (AIS), 10 with minimally invasive adenocarcinoma (MIA), and 51 with stage I invasive cancers. Additionally, three patients underwent neoadjuvant immuno-chemotherapy and tumor tissue specimens before and after treatment were obtained.

Results: Patients with stage I invasive cancer had significantly higher density ($P=0.01$) and percentage ($P=0.02$) of CD8⁺ T cells and higher percentages of M1 macrophages ($P=0.04$) and immature natural killer (NK) cells ($P=0.041$) in the tumor parenchyma compared to those with AIS/MIA. Patients with mutated epidermal growth factor receptor (*EGFR*) gene exhibited decreased NK cell infiltration, increased M2 macrophage infiltration, and decreased aggregation of CD4⁺ T cells near tumor cells compared to *EGFR* wild-type patients. As NSCLC progressed from stage I to III, CD8⁺ T cell density and proportion increased, while PD-L1⁺ tumor cells were in closer proximity to PD-1⁺CD8⁺ T cells, potentially inhibiting CD8⁺ T cell function. Furthermore, M1 macrophages decreased in density and proportion, and the number of NK cells, macrophages, and B cells around tumor cells decreased. Additionally, patients with tertiary lymphoid structures (TLSs) had significantly higher proportion of M1 macrophages and lymphocytes near tumor cells, whereas those without TLS had PD-L1⁺ tumor cells more densely clustered around PD-1⁺CD8⁺ T cells. Notably, neoadjuvant immuno-chemotherapy induced the development of TLS.

Conclusions: This study offers an in-depth analysis of immune changes in NSCLC, demonstrating

that the transition from AIS/MIA to invasive stage I NSCLC leads to immune activation, while the advancement from stage I to stage III cancer results in immune suppression. These findings contribute to our understanding of the molecular mechanisms underlying early-stage NSCLC progression and pave the way for the identification of potential treatment options.

Keywords: Non-small cell lung cancer (NSCLC); adenocarcinoma in situ (AIS); minimally invasive adenocarcinoma (MIA); tumor immune microenvironment (TIME); multiplex immunofluorescence technology (mIF technology)

Submitted Apr 29, 2024. Accepted for publication Aug 29, 2024. Published online Sep 20, 2024.

doi: 10.21037/tlcr-24-379

View this article at: <https://dx.doi.org/10.21037/tlcr-24-379>

Introduction

Non-small cell lung cancer (NSCLC) is the predominant type of lung cancer, accounting for 80–85% of all lung cancer cases. The recurrence and metastasis rates in early-

stage NSCLC patients range from 14.3% to 25.9% (1). Studies have demonstrated that invasive cancer cells usually spread early (T ≤4 cm, N0, M0), forming micrometastases as circulating tumor cells in the bloodstream or disseminated cancer cells in distant tissues, which subsequently develop into obvious distant metastases (2-4). Understanding the mechanisms of early-stage NSCLC progression and identifying key molecular markers can aid in accurately identifying patients at high risk of disease recurrence (5-13).

The evolution of lung cancer involves the progressive accumulation of molecular abnormalities and escape from immune surveillance, a process known as immunoediting. During the early stages of cancer development, the immune system recognizes and eliminates tumor cells through dynamic interactions with tumor cells. However, some tumor cells can acquire genomic mutations that enable them to evade immune surveillance, ultimately resulting in immune escape and tumor progression. It may be beneficial to intervene in the tumor immune microenvironment (TIME) of early-stage lung cancer patients before immune suppression and tumor escape are enhanced. Previous research has proposed interventions to prevent lung cancer by altering the immune microenvironment of the lungs (14). Tumor-infiltrating lymphocytes serve as supplementary indicators for the prediction of early recurrence and survival in NSCLC. For instance, the presence of CD8 cells portends a more favorable prognosis in early-stage lung cancer, whereas M2 macrophages, conversely, signal a poorer prognosis (15,16). Investigating the genomic and immune landscapes at different stages of early-stage lung cancer may shed light on the key time points of immune activation/escape during early lung cancer evolution and the underlying molecular mechanisms. Several studies have explored the immune evolution from preneoplasia to invasive lung cancer and identified underlying molecular

Highlight box

Key findings

- We investigated the changes in the tumor immune microenvironment during the evolution of early-stage lung cancer (adenocarcinoma in situ/minimally invasive adenocarcinoma to stage I invasive cancer) and explored immune changes driven by epidermal growth factor receptor (*EGFR*) mutations and neoadjuvant immuno-chemotherapy using multiplex immunofluorescence.

What is known and what is new?

- The tumor immune environment (TIME) is recognized for its dynamic nature and is acknowledged to significantly influence the diagnosis and prognosis of tumors.
- Our research introduces novel insights into the specific immune cell dynamics during the transition from precancerous lesions to invasive stage I non-small cell lung cancer (NSCLC), noting a marked increase in immune activation, especially among CD8⁺ T cells and M1 macrophages. Furthermore, we reveal that the progression to stage III NSCLC is characterized by a rise in immune suppression, evidenced by the interaction between PD-L1⁺ tumor cells and PD-1⁺CD8⁺ T cells. Additionally, we report the impact of *EGFR* mutation status on immune cell infiltration patterns and TIME, as well as the discovery that neoadjuvant immuno-chemotherapy can induce the formation of tertiary lymphoid structures, offering new avenues for NSCLC treatment strategies.

What is the implication, and what should change now?

- This research offers valuable insights into the alterations in the immune microenvironment of early-stage lung cancer and the underlying mechanisms of immune therapy, which can potentially influence decisions regarding clinical treatment options.

features (17-21). For instance, Dejima *et al.* reported that immune cytotoxicity decreases and immune escape increases during the tumor evolution from preneoplasia to invasive lung adenocarcinomas. Specifically, they found a decrease in cytotoxic T lymphocyte and anti-tumor helper T cell infiltration, an increase in regulatory T cell infiltration, and an upregulation of inhibitory checkpoint molecules programmed death ligand-1 (PD-L1) and cytotoxic T-lymphocyte-associated protein 4 (CTLA4) (17). However, a report contradicts these findings, indicating positivity rate of CD8 immunohistochemistry staining was higher in invasive lung adenocarcinoma, while the level of PD-L1 remains unchanged (18). It is to be noted that previous studies have primarily focused on analyzing specific immune cell density and proportion, neglecting the roles and spatial distribution of other immune cells within the TIME (17,18).

Therefore, in this study, we employed multiplex immunofluorescence (mIF) and next-generation sequencing (NGS) methods to evaluate the density and percentage of multiple immune cells and the spatial proximity of specific immune cells and lung cancer cells. Immune cell density was quantified as the number of positively stained cells per mm², while immune cell percentage was calculated as the ratio of specific cell types to the total number of cells identified by 4',6-diamidino-2-phenylindole (DAPI) staining. This allowed us to investigate changes in the TIME during the evolution of early-stage lung cancer [adenocarcinoma in situ (AIS)/minimally invasive adenocarcinoma (MIA) to stage I invasive cancer] and explore immune changes driven by specific gene mutations. Additionally, we examined the transition of infiltrating immune cells during the development of NSCLC (stage I to II to III). By adopting this comprehensive approach, we hope to contribute to a better understanding of the mechanisms of tumor evolution in early-stage lung cancer progression and provide insights into possible intervention strategies to improve patient outcomes. We present this article in accordance with the MDAR reporting checklist (available at <https://tclr.amegroups.com/article/view/10.21037/tclr-24-379/rc>).

Methods

Study design and patient populations

This study was designed to characterize the changes in the TIME underlying the onset and progression of NSCLC. We conducted a retrospective review of NSCLC patients who underwent a complete resection at the Affiliated

Hospital of Nantong University and Jinling Hospital between June 2017 and March 2023. The inclusion criteria were (I) patients between the ages of 18 and 90 years, male or female; (II) patients diagnosed with AIS, MIA, or invasive NSCLC, according to the 2015 World Health Organization (WHO) classification (22); and (III) patients had available tumor tissue specimens. The exclusion criteria were as follows: (I) patients with formalin-fixed paraffin-embedded (FFPE) tumor tissue block that was older than 5 years; and (II) patients with FFPE containing less than 20% tumor cell content. After applying both inclusion and exclusion criteria, 105 patients with NSCLC were included in the study. The cancer clinical stage was defined based on the 8th edition of the American Joint Committee on Cancer (AJCC) tumor-node-metastasis (TNM) stage system. For patients who received neoadjuvant therapy, both pre-treatment biopsy samples and surgical resection samples were collected. All the samples were subjected to mIF to assess the TIME. Additionally, to investigate the relationship between TIME changes and gene mutations in the early onset of NSCLC, NGS analysis was conducted on tumor samples obtained from patients with pre-cancerous lesions or stage I NSCLC. The study design flow diagram is presented in *Figure 1*. The study was conducted in accordance with the Declaration of Helsinki (as revised in 2013). The study was approved by the institutional ethics committee of the Affiliated Hospital of Nantong University (No. 2022-L144) and informed consent was taken from all the patients. Jinling Hospital was informed and agreed with this study.

DNA and RNA preparation and NGS

In our assay, DNA and RNA were co-extracted, co-constructed into libraries, and simultaneously sequenced. Through specialized primer design, the RNA and DNA results can be distinguished during the data analysis phase. Specifically, DNA and RNA were isolated from the same tumor tissue samples prepared as FFPE section curls or sections on slides. The amount of DNA and RNA in each sample was quantified, and if they met the minimum required amounts for the test, complementary DNA (cDNA) was synthesized from the RNA. For tissue-based targeted panel sequencing, indexed libraries were subjected to probe-based hybridization with a customized NGS panel targeting 35 cancer-related genes frequently rearranged genes. The mixture of extracted DNA and synthesized cDNA was loaded into the library cartridge provided in

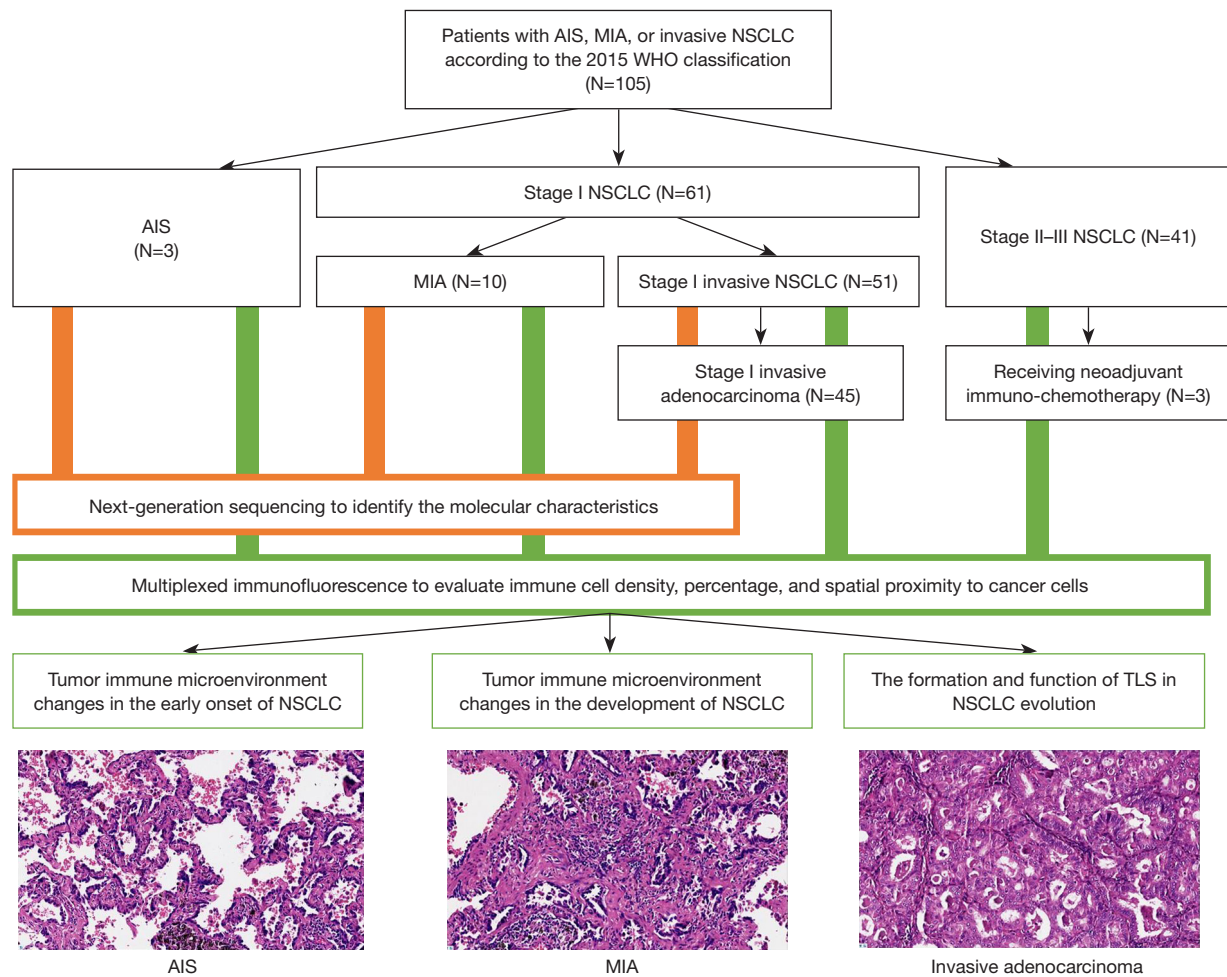


Figure 1 Flowchart depicting the overall design of the study. Example of HE staining of NSCLC tissues in the AIS, MIA, and invasive adenocarcinoma group (200 \times). AIS, adenocarcinoma in situ; MIA, minimally invasive adenocarcinoma; NSCLC, non-small cell lung cancer; WHO, World Health Organization; TLS, tertiary lymphoid structure; HE, hematoxylin and eosin.

the 3DMed OncoTM Core Tissue Kit (3D Medicines, Inc., Shanghai, China), which utilizes the RNase H-dependent polymerase chain reaction (PCR) technology (rhAmp PCR). This technology leverages the intrinsic properties of the RNase H2 enzyme and RNA-based-containing blocked primers, minimizing the formation of primer dimers and enabling the rhAmpSeq panels to be highly multiplexed. Subsequently, the library cartridge was loaded into the Automated NGS Prep System ANDiS 500 Instrument (3D Medicines, Inc.) for amplicon library preparation. The workflow of the amplicon library preparation involved two rounds of PCR amplification and purification. During the first PCR amplification, the target regions were amplified using specific rhAmp primers. Following the completion

of the first amplification, the amplicons were purified with magnetic beads. In the second PCR amplification step, the index primers containing sample indexes and P5/P7 sequences were appended to the rhAmp PCR amplicons (PCR 1 amplicons), followed by purification with magnetic beads. This workflow was applied to prepare the amplicon libraries of both positive and negative controls. The yield of each indexed amplicon library was quantified and normalized for a library pool, which was subsequently sequenced using the Illumina Sequencing platform (Illumina, Inc., San Diego, CA, USA). For microsatellite instability (MSI) analysis, a total of 100 microsatellite loci were selected to determine MSI status. The MSI score was defined as the percentage of unstable loci. Samples with

an MSI score of ≥ 0.4 were classified as MSI, and otherwise MSS. 3D Med's inhouse-developed software TiNAiLab (a sequence data analytics platform) was utilized to analyze the sequencing data and generate reports containing a summary of samples, test results with detected variants, MSI status from DNA sequencing data, and gene fusions from RNA sequencing data (Table S1).

mIF

FFPE lung cancer tissue sections were analyzed to investigate the TIME using previously described methods by 3D Medicines, Inc.) (23,24). Primary antibodies against specific markers, including CD163, CD68, PD-1, PD-L1, CD3, CD4, CD8, CD56, CD20, Foxp3, and pan-cytokeratin (pan-CK), were sequentially applied to the FFPE tissue slides (Table S2). After incubation with secondary antibodies, corresponding reactive Opal fluorophores, and DAPI, the multiplex-stained slides were scanned using a Vectra Polaris Quantitative Pathology Imaging System (Akoya Biosciences, Marlborough, MA, USA). All scans for each slide were superimposed to generate a single image. Fluorescence images were analyzed using the APTIME software developed by 3D Medicines. Tumor parenchyma and stroma were differentiated based on CK staining. The quantities of immune cell subsets in tumor and stroma regions were determined by detecting specific marker expression, including CD3⁺, CD3⁺CD4⁺, CD8⁺, CD20⁺, Foxp3⁺, PD-1⁺, PD-1⁺CD8⁺, CD3⁺CD4⁺Foxp3⁺, CD68⁺CD163⁻ (M1 macrophage), CD68⁺CD163⁺ (M2 macrophage), PD-L1⁺CD68⁺, CD56^{bright} [immature natural killer (NK) cell], and CD56^{dimm} (mature NK cell). The presence of both CD3⁺ T cells and CD20⁺ B cells indicates the formation of tertiary lymphoid structures (TLSs). These cell subsets were analyzed for both density (number of stained cells per square millimeter) and percentage (proportion of positively stained cells among all nucleated cells). Additionally, spatial analysis was performed to examine the spatial relationship between immune cells and tumor cells by calculating the average number of cells within a proximity distance of 30 μm in the condition that both immune and tumor cells are present.

Statistical analysis

Differences between the two groups were assessed using the Mann-Whitney *U* test for continuous variables, Fisher's exact test for binary variables, and the chi-square test for

multi-categorical variables. All reported P values were two-tailed, and a P value of <0.05 was considered statistically significant unless otherwise stated. Statistical analyses were performed using R software, version 3.6.1 (R Foundation for Statistical Computing, Vienna, Austria), and Python software, version 3.9.5. As this was a descriptive study, no formal sample size calculation was performed and the sample size was based on the availability of samples.

Results

Clinical, pathologic, and molecular characteristics

A total of 105 NSCLC patients were included in the study, the majority of whom had adenocarcinoma ($n=84$, 80.0%). The median age of the patients was 65 years, with a range of 30 to 81 years, and 61 (58.1%) were male. The detailed baseline characteristics of these patients are provided in Table 1. Of these 105 patients, three were diagnosed with AIS, 10 with MIA (stage I), 51 with IAC (stage I), 12 with stage II, and 29 with stage III. Adenocarcinoma accounted for 90.2% (55/61) in stage I, 66.7% (8/12) in stage II, and 62.1% (18/29) in stage III. Among the 61 patients with stage I cancer, 10 had MIA, while 51 had invasive lung cancer consisting of 45 cases of adenocarcinoma, three cases of squamous cell carcinoma, and one case each of adenosquamous carcinoma, carcinoid, and large cell carcinoma. Of the 41 patients with stage II–III disease, three received neoadjuvant immuno-chemotherapy, and two patients had a pathologic complete response (pCR).

NGS testing data were available for a subset of 64 patients, including three with AIS, 10 with MIA, and 51 with stage I invasive disease. Epidermal growth factor receptor (*EGFR*) mutations were observed in eight out of 13 patients (61.5%) with AIS/MIA and in 38 out of 51 patients (74.5%) with stage I invasive cancer (Figure 2). The prevalence of other tumor-related gene mutations (such as *ALK*, *KRAS*, *BRAF*) was below 10% in both the AIS/MIA and stage I invasive cancer patients, with no significant difference between the two groups.

TIME changes in the early onset of NSCLC

Using mIF, we performed the staining for multiple immune cell markers on tumor tissue samples. The cell density and proportion in the malignant cell areas and adjacent stromal areas of 64 patients with AIS/MIA or stage I invasive cancer are displayed in a heatmap (Figure S1). We compared the

Table 1 Clinicopathological characteristics of patients

Characteristics	Values (n=105)
Age (years)	65 [30–81]
Sex	
Male	61 (58.1)
Female	44 (41.9)
Stage	
0	3 (2.9)
I	61 (58.1)
II	12 (11.4)
III	29 (27.6)
Histology	
Adenocarcinoma	84 (80.0)
Squamous cell carcinoma	16 (15.2)
Carcinoid	1 (1.0)
Large cell carcinoma	1 (1.0)
Adenosquamous carcinoma	2 (1.9)
Mucinous adenocarcinoma	1 (1.0)
Histopathology	
AIS	3 (2.9)
MIA	10 (9.5)
Invasive cancer	92 (87.6)
Smoking status	
Yes	49 (46.7)
No	56 (53.3)

Values are presented as median [range] or n (%). AIS, adenocarcinoma in situ; MIA, minimally invasive adenocarcinoma.

differences in immune cell infiltration between AIS/MIA and stage I invasive cancer patients. The results showed that patients with stage I invasive cancer had significantly higher density ($P=0.01$) and percentage ($P=0.02$) of CD8⁺ T cells in the tumor parenchyma compared to patients with AIS/MIA (Figure 3A, 3B). Additionally, patients with stage I invasive cancer exhibited significantly higher percentages of M1 macrophages ($P=0.04$) and immature NK cells ($P=0.041$) in the tumor parenchyma compared to AIS/MIA patients (Figure 3C, 3D). There were no significant differences in the density and proportion of other immune cell subsets in both the tumor and stroma regions between the two groups (Figure S2). Furthermore, we observed that 15.4% (2/13)

of the AIS/MIA patients had TLS, while 49.02% (25/51) of the patients with stage I invasive NSCLC had TLS, representing a significant increase ($P=0.03$) (Figure 3E).

In addition to analyzing the density and proportion of immune cells, we also performed spatial analysis to assess the average number of various immune cells in close proximity ($\leq 30 \mu\text{m}$) to a tumor cell or a PD-L1⁺ tumor cell. There were no significant differences between patients with AIS/MIA and stage I invasive NSCLC for any immune cell subsets (Figure S3). These results collectively indicated that immune evolution progressed from AIS/MIA to stage I invasive disease with a modest enhancement in immunity.

We also compared immune cell infiltration of the tumor parenchyma and stroma between *EGFR*-mutated and wild-type groups in 64 patients with AIS/MIA or stage I invasive cancer. Patients with *EGFR* mutations had a significantly lower density of immature NK cells in the tumor ($P=0.04$) and a lower percentage in both the tumor ($P=0.02$) and stroma ($P=0.04$) compared to those with wild-type *EGFR* (Figure 4A–4C). Similarly, patients with *EGFR* mutations had significantly lower density ($P=0.05$) and percentage ($P=0.03$) of mature NK cells in the stroma compared to those with wild-type *EGFR* (Figure 4D, 4E). Additionally, we found a significant increase in the density of M2 macrophages ($P=0.02$) in patients with *EGFR* mutations compared to those with wild-type *EGFR* in the tumor region (Figure 4F). No significant differences were observed in the quantity and proportion of other immune cell subsets among patients with *EGFR* mutations and those with wild-type *EGFR* status (Figure S4). Furthermore, the spatial analysis showed that the average number of CD4⁺ cells within 30 μm of a tumor cell was significantly lower in patients with *EGFR* mutations compared to those with wild-type *EGFR* ($P=0.03$) (Figure 4G, Figure S5). These data suggest that *EGFR*-mutated AIS/stage I patients had an overall decreased immunity compared to those with wild-type *EGFR*.

We conducted a further analysis to explore the differences in immune cell infiltration between smokers and non-smokers. The results indicated that smokers had a higher proportion of tumoral CD3⁺ T cells ($P=0.041$) and CD8⁺PD-1⁺ ($P=0.048$) cells compared to non-smokers (Figure S6).

Changes in the TIME during NSCLC development

The immune cell density and proportion in the tumor and stromal areas of 102 patients with stage I–III cancer were

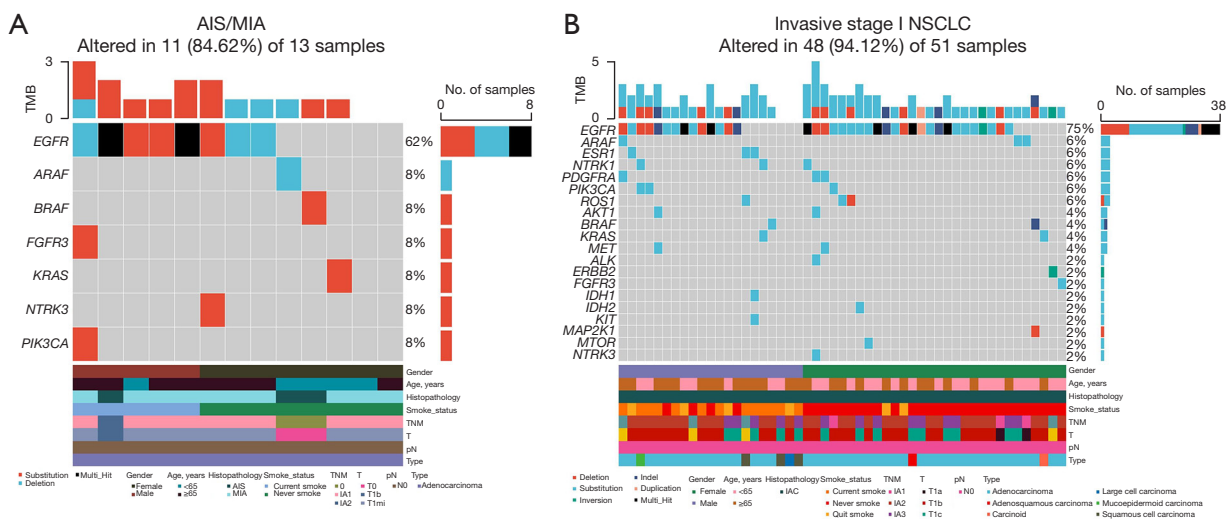


Figure 2 Heatmap demonstrating the mutational landscape of the primary tumors from patients with AIS/MIA (n=13) or invasive stage I NSCLC (n=51). AIS, adenocarcinoma in situ; MIA, minimally invasive adenocarcinoma; TMB, tumor mutational burden; TNM, tumor-node-metastasis; NSCLC, non-small cell lung cancer.

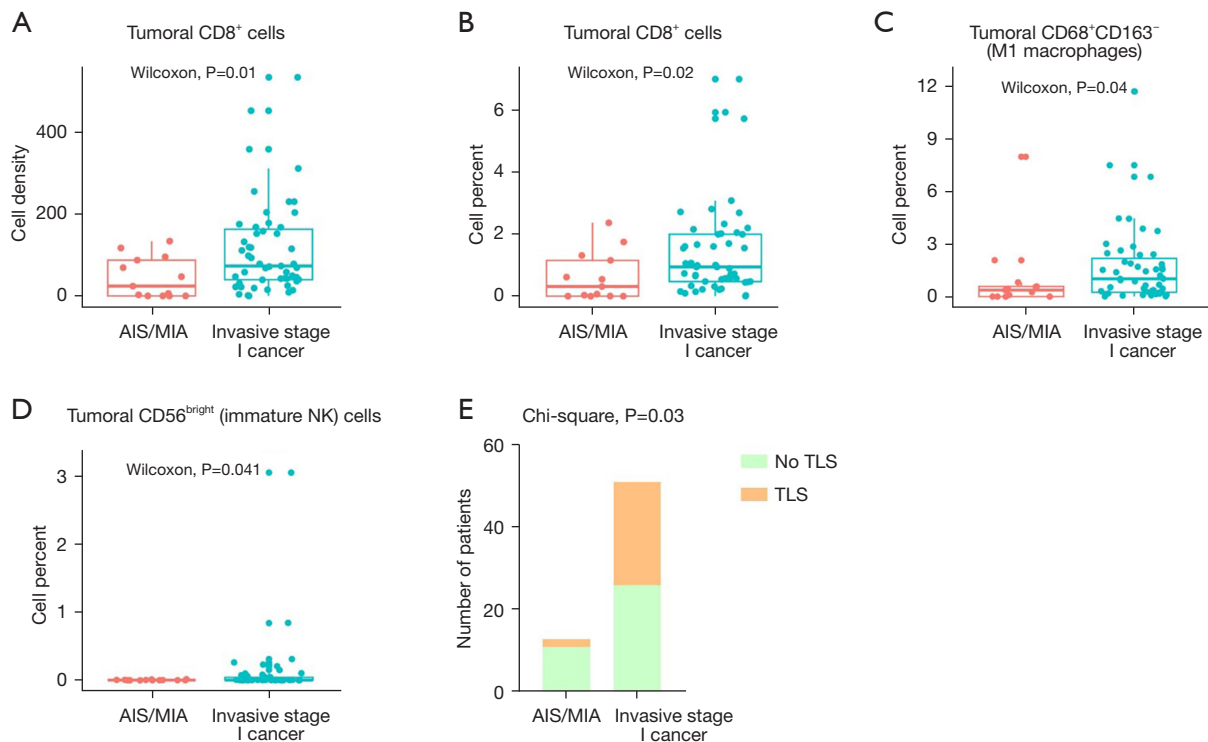


Figure 3 Changes in the TIME between AIS/MIA (n=13) and stage I invasive cancer patients (n=51). (A-E) Comparison of density of tumoral CD8⁺ T cells (A), percentage of tumoral CD8⁺ T cells (B), tumoral M1 macrophages (C), and tumoral immature NK cells (D), and the occurrence rate of TLS (E) between AIS/MIA and stage I invasive cancer samples. AIS, adenocarcinoma in situ; MIA, minimally invasive adenocarcinoma; NK, natural killer; NSCLC, non-small cell lung cancer; TLS, tertiary lymphoid structure; TIME, tumor immune microenvironment.

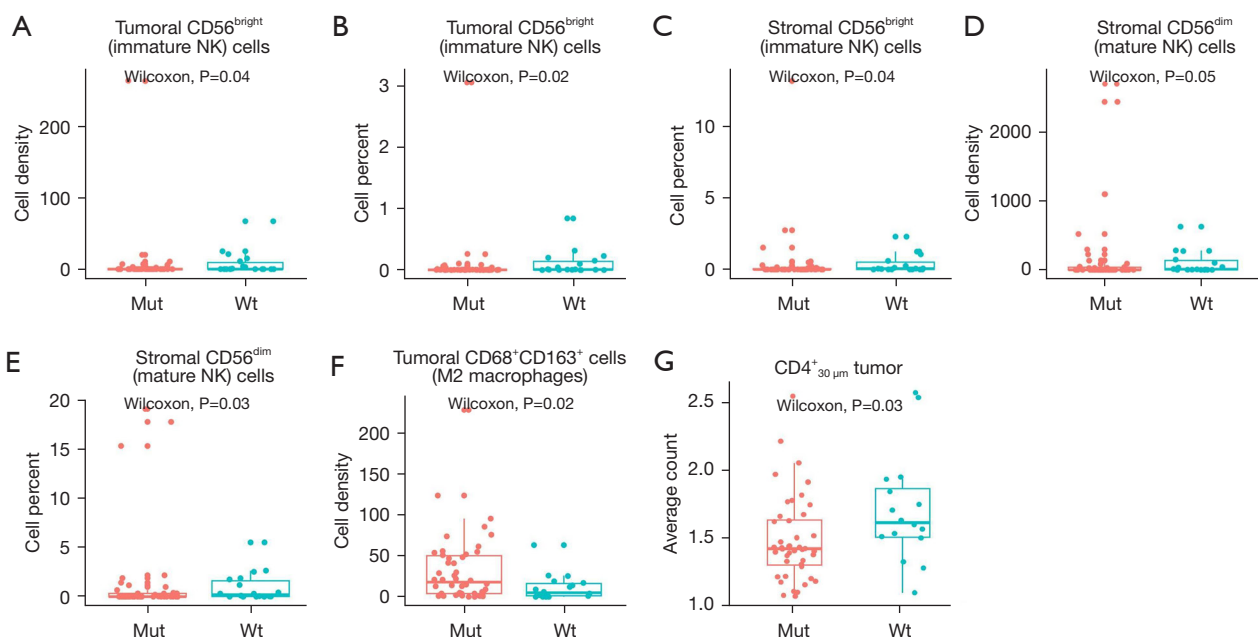


Figure 4 Comparison of the TIME between patients with *EGFR*-mutated (n=46) and wild-type AIS/stage I NSCLC (n=18). (A) Comparison of density of tumoral immature NK cells between patients with *EGFR*-mutated and wild-type AIS/stage I NSCLC. (B,C) Comparison of percentage of tumoral immature NK cells (B), stromal immature NK cells (C) between patients with *EGFR*-mutated and wild-type AIS/stage I NSCLC. (D) Comparison of density of stromal mature NK cells between patients with *EGFR*-mutated and wild-type AIS/stage I NSCLC. (E) Comparison of percentage of stromal mature NK cells between patients with *EGFR*-mutated and wild-type AIS/stage I NSCLC. (F) Comparison of density of tumoral M2 macrophages between patients with *EGFR*-mutated and wild-type AIS/stage I NSCLC. (G) Comparison of the average number of CD4⁺ T cells within 30 μm of a tumor cell between patients with *EGFR*-mutated and wild-type AIS/stage I NSCLC. Mut, mutated; Wt, wild-type; NK, natural killer; TIME, tumor immune microenvironment; *EGFR*, epidermal growth factor receptor; AIS, adenocarcinoma in situ; NSCLC, non-small cell lung cancer.

displayed in Figure S7. We observed that the density and proportion of CD8⁺ T cells increased with advancing tumor stages. The enrichment of CD8⁺ T cells in the stroma was more significant compared to the tumor parenchyma with increasing tumor stage (Figure 5A-5D). In stage III patients, the density (P=0.01) and percentage (P=0.01) of CD8⁺ T cells in the stroma were significantly higher than those in stage I patients (Figure 5B,5D). Conversely, M1 macrophages showed a decreasing trend during NSCLC development from stage I to II to III, and the proportion of M1 macrophages in the tumor parenchyma was significantly lower in stage III patients compared to stage I patients (P=0.03) (Figure 5E-5H). The density (P=0.06) and percentage (P=0.07) of immature NK cells in the tumor were also nearly significantly lower in stage III patients than in stage I patients (Figure 5I,5J). Other immune cells did not show significant differences with increasing tumor stage in both tumor and stroma regions (Figure S8).

TLS was observed in 44.3% (27/61) of stage I patients, 41.7% (5/12) of stage II patients, and 0% of stage III patients, showing a significant decrease with increasing stage (P<0.001) (Figure 5K).

Spatial analysis showed that during NSCLC progression, CD8⁺ T cells were enriched near the tumor cells (P=0.01), while PD-L1⁺ tumor cells were in closer proximity to PD-1⁺CD8⁺ T cells (P=0.01) (Figure 6A,6B). This suggests that despite increased CD8⁺ T cell infiltration near tumor cells during NSCLC progression, the function of CD8⁺ T cells might be inhibited by the PD-L1/PD-1 immune checkpoint. Furthermore, there was a significant decrease in natural anti-tumor immune cells such as NK cells (P=0.02), B cells (P=0.001), macrophages (P=0.03), and M1 macrophages (P=0.02) around tumor cells during NSCLC progression (Figure 6C-6F). No significant change was observed in CD3⁺ T cells and CD4⁺ T cells around tumor cells (Figure S9). These data collectively indicate that the

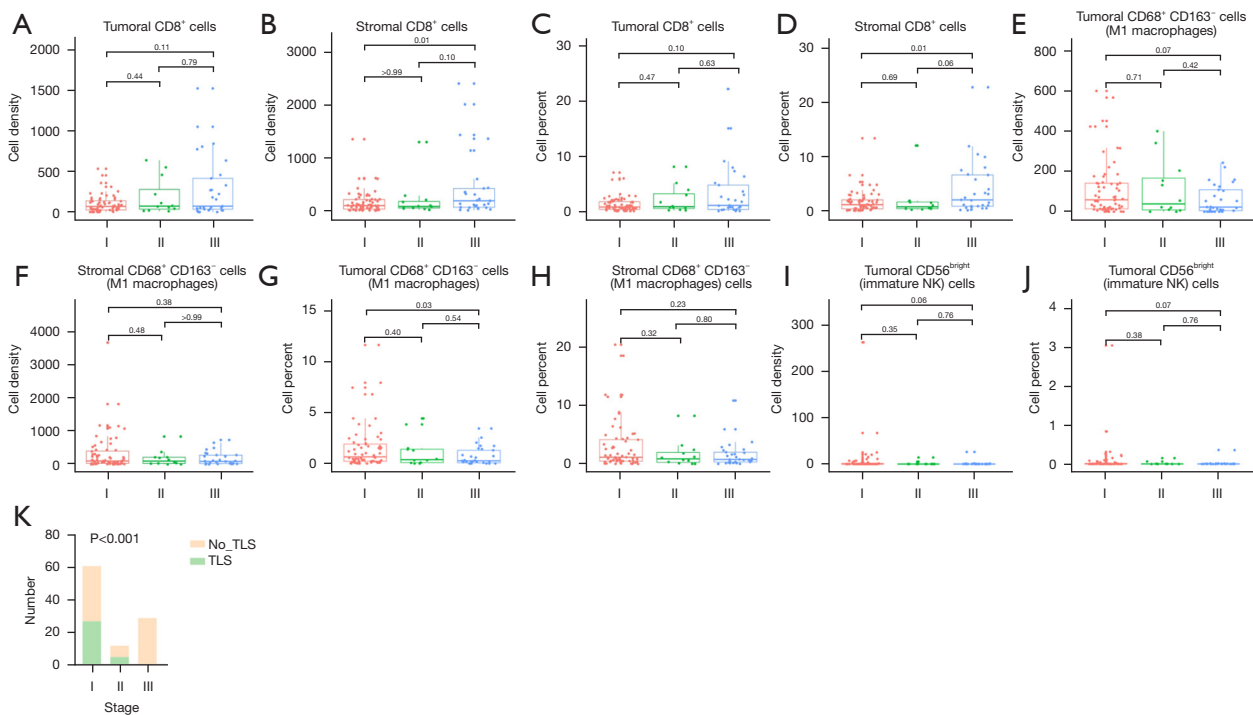


Figure 5 Changes in the density and percentage of immune cells in the TIME among patients with stages I, II, and III (n=102). (A,B) Comparison of density of tumoral CD8⁺ T cells (A), stromal CD8⁺ T cells (B) among patients with stage I, II and III. (C,D) Comparison of percentage of tumoral CD8⁺ T cells (C), stromal CD8⁺ T cells (D) among patients with stage I, II and III. (E,F) Comparison of density of tumoral M1 macrophages (E), stromal M1 macrophages (F) among patients with stage I, II, and III. (G,H) Comparison of percentage of tumoral M1 macrophages (G), stromal M1 macrophages (H) among patients with stage I, II and III. (I) Comparison of density of tumoral immature NK cells among patients with stage I, II, and III. (J) Comparison of percentage of tumoral immature NK cells among patients with stage I, II, and III. (K) Comparison of the occurrence rate of TLS among patients with stage I, II, and III. NK, natural killer; TLS, tertiary lymphoid structure; TIME, tumor immune microenvironment.

progression from stage I to II to III represents an immune-suppressive process.

The formation and function of TLS in NSCLC evolution

Given that TLS, composed of T and B cell zones and germinal centers, was widely reported to be a strong biomarker of an immunologically 'hot' environment and indicator of immunotherapy efficacy, we focused on TLS formation and function during the NSCLC evolution. Our results above showed that the occurrence rate of TLS decreased with the increasing stage. Spatial analysis revealed a significant reduction in the clustering of CD20⁺ B cells around CD3⁺ T cells in stage III patients compared to stage I patients (P<0.001) (Figure 7A). Furthermore, we found that TLS-positive patients exhibited significantly higher aggregation of B cells near CD3⁺ T cells compared to

TLS-negative patients (P<0.001) (Figure 7B). These results suggest that B cells may play a crucial role in the formation of TLS, creating an environment that facilitates optimal interaction between T cells, B cells, and dendritic cells.

Additionally, when comparing TLS-positive and TLS-negative patients in NSCLC, we observed that TLS-positive patients had a significantly higher density (P=0.046) and proportion (P=0.041) of M1 macrophages in the tumor (Figure 8A,8B). No significant differences were found in other immune cell populations between TLS-positive and TLS-negative patients in both the tumor and stromal regions (Figure S10). Spatial analysis revealed that tumor cells were significantly more densely clustered with CD3⁺ T cells (P=0.03), CD4⁺ T cells (P=0.006), and CD20⁺ B cells (P<0.001) in TLS-positive patients compared to TLS-negative patients (Figure 8C-8E). Furthermore, TLS-positive patients had a lower aggregation of PD-L1⁺ tumor

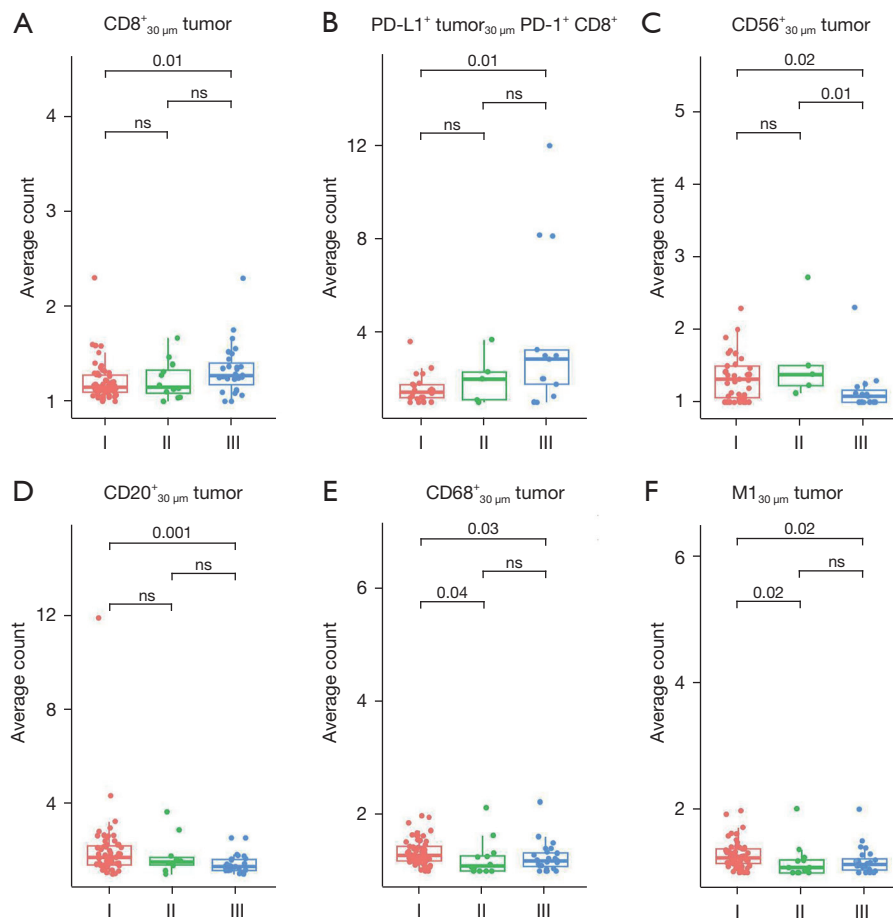


Figure 6 Changes in spatial proximity of lung cancer cells and specific immune cells in the TIME among patients with stages I, II, and III (n=102). (A) Comparison of the average number of CD8⁺ T cells within 30 μm of a tumor cell in the TIME among patients with stage I, II and III. (B) Comparison of the average number of tumor cells expressing PD-L1 within 30 μm of a PD-1⁺CD8⁺ T cell in the TIME among patients with stage I, II and III. (C-F) Comparison of the average number of CD56⁺ NK cells (C), CD20⁺ B cells (D), CD68⁺ macrophages (E), and M1 macrophages (F) within 30 μm of a tumor cell in the TIME among patients with stage I, II and III. TIME, tumor immune microenvironment; NK, natural killer; ns, not significant.

cells near PD-1⁺CD8⁺ immune cells than TLS-negative patients (P=0.01) (Figure 8F, Figure S11). These results collectively suggest that TLS formation is associated with a stronger immune-infiltrated TIME with anti-tumor activity.

Among the 41 patients with stage II–III disease, three patients received neoadjuvant immuno-chemotherapy. We analyzed samples from these patients before and after treatment to assess changes in TLS. Prior to treatment, TLS was not detected but became evident after treatment in these patients (Figure 9). As of August 1, 2022, the postoperative follow-up time was 36.8, 33.5, and 40.3 months for these three patients respectively, and none of them experienced relapse. This finding may underpin the

favorable efficacy of the combination therapy.

Discussion

In this study, we discovered significant differences in the immune profiles of patients with stage I invasive NSCLC compared to those with AIS/MIA. Specifically, patients with stage I invasive NSCLC exhibited higher density and percentage of CD8⁺ T cells in the tumor parenchyma. Additionally, they had higher percentages of M1 macrophages and immature NK cells, as well as a higher proportion of TLS, indicating immune system activation. Patients with *EGFR* mutations displayed a more suppressive

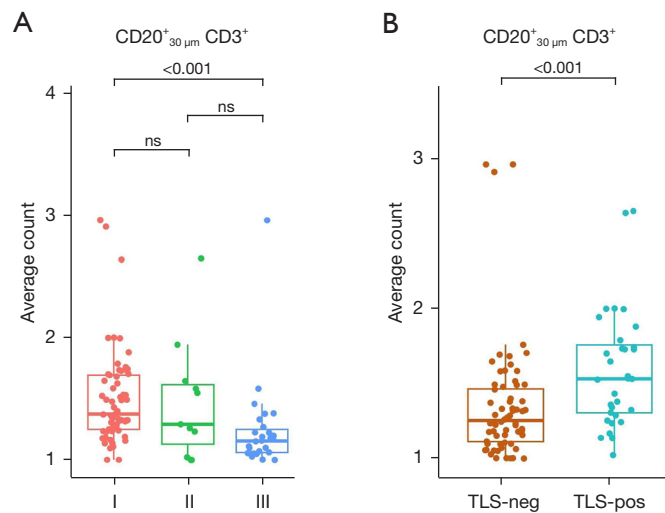


Figure 7 TLS formation is associated with the clustering of CD20⁺ B cells around CD3⁺ T cells. (A) Comparison of the average number of CD20⁺ B cells within 30 μm of a CD3⁺ T cell among patients with stage I, II, and III. (B) Comparison of the average number of CD20⁺ B cells within 30 μm of a CD3⁺ T cell between patients with or without TLS. TLS, tertiary lymphoid structure; neg, negative; pos, positive; ns, not significant.

immune microenvironment compared to those with *EGFR* wild-type. As NSCLC progressed pathologically, there was a noticeable increase in CD8⁺ T cell abundance. However, we observed that PD-L1⁺ tumor cells were in closer proximity to PD-1⁺CD8⁺ T cells which may hinder CD8⁺ T cell cytotoxicity through the PD-1/PD-L1 immune checkpoint. Additionally, there was a decreasing trend in M1 macrophages and TLS, as well as a gradual decrease in NK cells and B cells near tumor cells. These findings suggest that as the tumor progresses, a more suppressive TIME emerges, emphasizing the dynamic interplay between tumor cells and the host immune surveillance, and leading to immune escape.

The pathological evolution of lung cancer is a highly intricate process (Figure S12), in which changes in the TIME may play a crucial role. Previous studies have shown that as lung cancer progresses, the number and function of various immune cells infiltrating the TIME, particularly T cells, undergo changes. For instance, research by Zhang *et al.* investigated the genomic landscape and immune microenvironment features of preinvasive and early invasive lung adenocarcinoma, revealing an increasing trend in CD8⁺ T cells from AIS to MIA to invasive adenocarcinoma (18). Similarly, Wang *et al.* conducted single-cell RNA sequencing on tumor and normal samples, finding that CD8⁺ T cells were enriched in the tumor during tumor progression. However, they also observed the expression

of human leukocyte antigen-DR alpha (HLA-DRA), an exhaustion marker, in CD8⁺ T cells (19). Consistent with these findings, our study confirmed an increase in CD8⁺ T cell density and percentage as lung cancer progressed from AIS/MIA to invasive stage I and from stage I to III. However, we also observed an increasing aggregation of PD-L1⁺ tumor cells near PD-1⁺CD8⁺ T cells in stages I–II–III. The interaction between PD-L1⁺ tumor cells and PD-1⁺CD8⁺ T cells through the PD-L1/PD-1 binding pathway can suppress T cell proliferation, cytokine production, and cytotoxicity, which are crucial for effective anti-tumor immune responses. This interaction promotes the evasion of immune surveillance and sustained growth of tumors.

NK cells, which play important roles in innate immunity, are known for their anti-tumor, antiviral, and antimicrobial activities, as well as their contributions to the activation and regulation of adaptive immune responses. NK cells consist of immature and mature subsets, with immature NK cells exhibiting limited functionality and undergoing maturation in the bone marrow, while mature NK cells possess potent cytotoxic and cytokine production abilities. Previous studies have yielded inconsistent results regarding the changes in NK cells during tumor evolution. For example, Zhu *et al.* (20) analyzed the dynamic evolution from preneoplasia to invasive lung adenocarcinoma and found that the percentage of NK cells increased from AIS to MIA, but then decreased from MIA to invasive

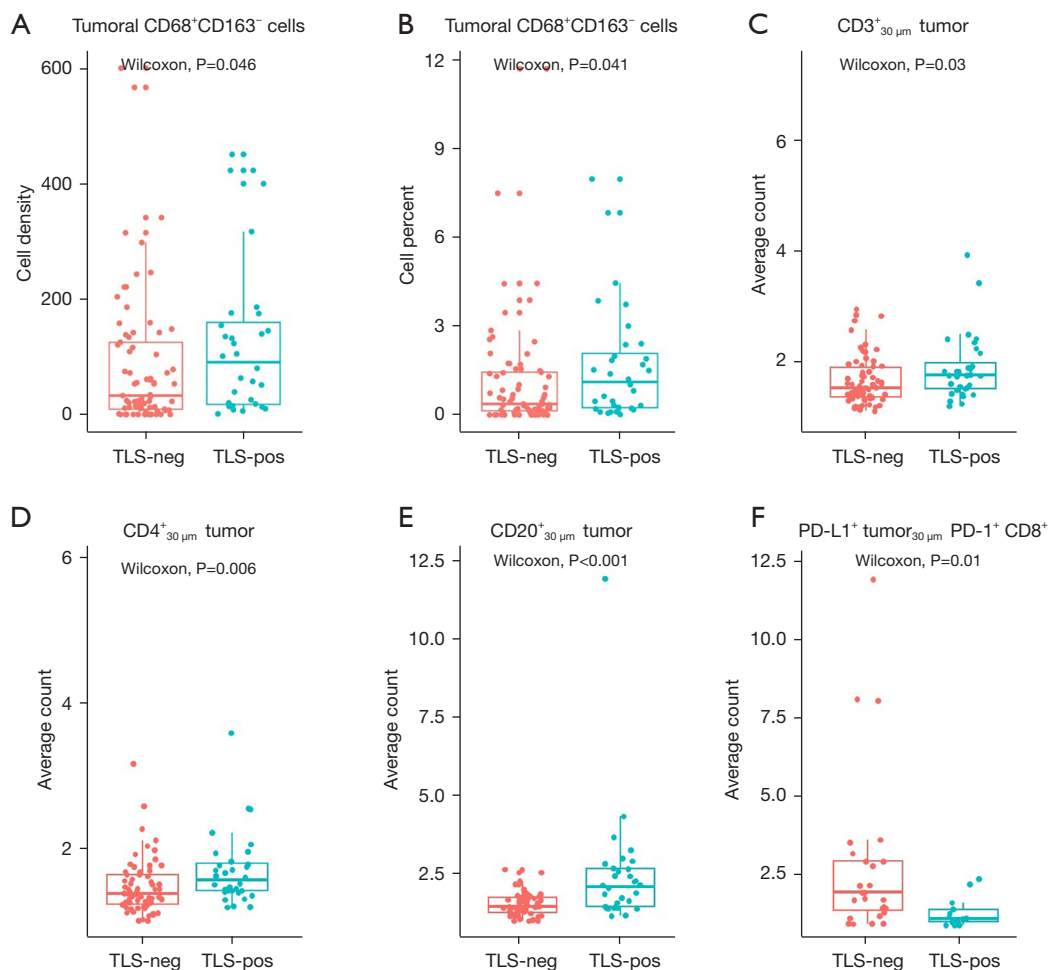


Figure 8 Changes in the TIME between patients with or without TLS (n=102). (A,B) Comparison of density (A) and proportion (B) of tumoral M1 macrophages between patients with or without TLS. (C-F) Comparison of the average number of CD3⁺ T cells (C), CD4⁺ T cells (D), and CD20⁺ B cells (E) within 30 µm of a tumor cell and tumor cells expressing PD-L1 (F) within 30 µm of a PD-1⁺CD8⁺ T cell in the TIME between patients with or without TLS. TLS, tertiary lymphoid structure; neg, negative; pos, positive; TIME, tumor immune microenvironment.

adenocarcinoma. In contrast, Wang *et al.* found that NK cells decreased from AIS to MIA, but remained unchanged from MIA to invasive lung adenocarcinoma (25). In our study, we focused on the changes in both immature and mature NK cell abundance in response to tumor evolution. We observed a nearly significant decrease in immature NK cell abundance as the disease progressed from stage I to III, but no changes were observed in the early stages from AIS/MIA to stage I invasive cancer. These findings might suggest a dysregulation or impairment in the differentiation and maturation of NK cells in the middle-to-late-stage development of the disease. Previous studies have indicated

that disruptions to the differentiation and maturation process of NK cells may be influenced by tumor evasion mechanisms and immunosuppressive factors in the TIME (26-28).

According to a recent study, macrophages are the most abundant immune cell type in lung cancer, accounting for 13.39% of all cells (29). Macrophages exist in two activation stages: M1 and M2. M1 macrophages possess tumor-antagonizing functions by producing proinflammatory cytokines and reactive oxygen/nitrogen species to kill tumor cells. In contrast, M2 macrophages promote tumor growth by producing anti-inflammatory cytokines and suppressing immunosurveillance (30,31). Our study

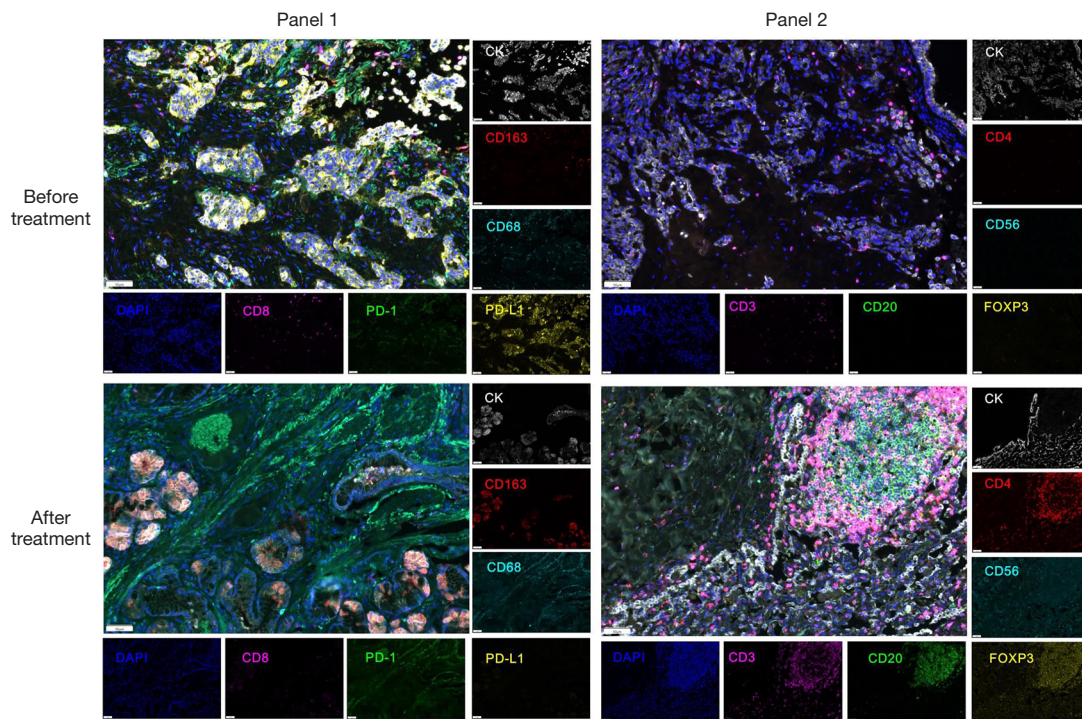


Figure 9 Neoadjuvant immuno-chemotherapy facilitates the formation of TLSs. There were three patients with stage II or III NSCLC who underwent neoadjuvant immuno-chemotherapy. The tumor tissue specimens before and after neoadjuvant treatment were subjected to mIF and images of the representative mIF results are shown. TLS is displayed in the lower right panel. First row: pre-neoadjuvant therapy mIF images; second row: post-neoadjuvant surgery mIF images. The scale bar represented 50 μ m. Samples were stained using an Opal automation mIF Detection Kit (Akoya). A total of 11 markers were labeled in two seven-color multiplex panels. DAPI, 4',6-diamidino-2-phenylindole; CK, cytokeratin; TLS, tertiary lymphoid structure; NSCLC, non-small cell lung cancer; mIF, multiplex immunofluorescence.

demonstrated that M1 macrophages increased from AIS/MIA to stage I invasive cancer, but decreased from stage I to stage III. TLS, which indicates an immunologically 'hot' environment, exhibited a consistent trend with M1 macrophages, with an initial increase followed by subsequent decrease. Additionally, NK cells and B cells near tumor cells gradually decreased from stage I to stage III. These results suggest that the transition from AIS/MIA to stage I invasive cancer is an immune-activating process where immune cells are activated and seek out to eliminate tumor cells, while the progression from stage I to stage III represents an immune-suppressive process, where tumor cells employ various mechanisms to evade attack by the immune system. *EGFR*-mutated lung cancer is known to have an immune-deprived microenvironment characterized by increased immunosuppressive cytokines and regulatory T cell infiltration (32,33). Our study provided consistent evidence that *EGFR*-mutated patients displayed a more pronounced immunosuppressive microenvironment

compared to *EGFR* wild-type patients.

The formation of TLS is a dynamic process starting with sparse lymphocytic infiltrates that evolve into aggregates and eventually organize into distinct T cell areas and B cell follicles with germinal centers (34,35). TLS-B cells limit the production of CD4⁺ regulatory T cells while promoting the activation of CD4⁺ T cells and inhibiting the exhaustion of CD4⁺ T cells, thus actively regulating anti-tumor T cell immunity (36). Several recent studies have considered TLS as an independent favorable prognostic factor, and high-density TLS is associated with a low lymphatic metastasis rate (37-39). Therefore, promoting TLS formation may significantly improve the survival prognosis of NSCLC patients. In our study, we found that the formation of TLS is associated with the clustering of CD20⁺ B cells around CD3⁺ T cells. TLS-positive patients have a TIME with stronger anti-tumor activity, as evidenced by significantly higher M1 abundance in the tumor, and significantly more CD3⁺ T cells, CD20⁺ B cells, and CD4⁺ T cells near

tumor cells. Patients without TLS have significantly closer proximity between PD-1⁺CD8⁺ immune cells and PD-L1⁺ tumor cells compared to patients with TLS, indicating stronger inhibition of CD8⁺ T cell cytotoxicity through the PD-1/PD-L1 immune checkpoint. Immunotherapy can alleviate the inhibitory effects of the PD-1/PD-L1 immune checkpoint and promote TLS formation. In our study, neoadjuvant immuno-chemotherapy was found to promote TLS formation and facilitate an active immune microenvironment, which may greatly promote patient survival.

First, this study was limited by its retrospective design and small sample size. Second, only a limited number of immune markers was assessed. Nevertheless, the use of mIF allowed for the characterization of multiple biomarkers that are closely related to immune activators and suppressors, making it feasible to monitor the TIME during tumor evolution. Future studies should integrate analysis from diverse confirmatory experimental methods, including messenger RNA (mRNA) sequencing, whole-exome sequencing, and immunoproteomics.

Conclusions

This study revealed that as NSCLC progresses toward malignancy, there is an increasing trend of CD8⁺ T cell infiltration and TLS, indicating immune activation. However, during the transition from early-stage malignancy to middle-to-late-stage malignancy, although CD8⁺ T cell infiltration increases, its cytotoxic functions might be suppressed by PD-L1/PD-1 binding. At this stage, immunotherapy can effectively relieve immune suppression and yield positive therapeutic outcomes (40-42). TLS shows a direct reduction trend during NSCLC progression from stage I to III but can increase after immuno-chemotherapy. This study provides important insights into the changes in the immune microenvironment of early-stage lung cancer and the mechanisms of immune therapy.

Acknowledgments

The authors would like to acknowledge the patients who participated in this study.

Funding: None.

Footnote

Reporting Checklist: The authors have completed the MDAR

reporting checklist. Available at <https://tcr.amegroups.com/article/view/10.21037/tcr-24-379/rc>

Data Sharing Statement: Available at <https://tcr.amegroups.com/article/view/10.21037/tcr-24-379/dss>

Peer Review File: Available at <https://tcr.amegroups.com/article/view/10.21037/tcr-24-379/prf>

Conflicts of Interest: All authors have completed the ICMJE uniform disclosure form (available at <https://tcr.amegroups.com/article/view/10.21037/tcr-24-379/coif>). Y.S. serves as an Editor-in-Chief of *Translational Lung Cancer Research*. D.Z., J.C., B.Z., Junling Zhang, and M.H. are from 3D Medicines Inc. The other authors have no other conflicts of interest to declare.

Ethical Statement: The authors are accountable for all aspects of the work in ensuring that questions related to the accuracy or integrity of any part of the work are appropriately investigated and resolved. The study was conducted in accordance with the Declaration of Helsinki (as revised in 2013). The study was approved by the institutional ethics committee of the Affiliated Hospital of Nantong University (No. 2022-L144), and informed consent was taken from all the patients. Jinling Hospital was informed and agreed with this study.

Open Access Statement: This is an Open Access article distributed in accordance with the Creative Commons Attribution-NonCommercial-NoDerivs 4.0 International License (CC BY-NC-ND 4.0), which permits the non-commercial replication and distribution of the article with the strict proviso that no changes or edits are made and the original work is properly cited (including links to both the formal publication through the relevant DOI and the license). See: <https://creativecommons.org/licenses/by-nc-nd/4.0/>.

References

1. Dai L, Yan W, Kang X, et al. Exploration of Postoperative Follow-up Strategies for Early Staged NSCLC Patients on the Basis of Follow-up Result of 416 Stage I NSCLC Patients after Lobectomy. *Zhongguo Fei Ai Za Zhi* 2018;21:199-203.
2. Herbst RS, Morgensztern D, Boshoff C. The biology and management of non-small cell lung cancer. *Nature* 2018;553:446-54.

3. Goldstraw P, Chansky K, Crowley J, et al. The IASLC Lung Cancer Staging Project: Proposals for Revision of the TNM Stage Groupings in the Forthcoming (Eighth) Edition of the TNM Classification for Lung Cancer. *J Thorac Oncol* 2016;11:39-51.
4. Lambert AW, Pattabiraman DR, Weinberg RA. Emerging Biological Principles of Metastasis. *Cell* 2017;168:670-91.
5. Maynard A, McCoach CE, Rotow JK, et al. Therapy-Induced Evolution of Human Lung Cancer Revealed by Single-Cell RNA Sequencing. *Cell* 2020;182:1232-1251.e22.
6. Rosenthal R, Cadieux EL, Salgado R, et al. Neoantigen-directed immune escape in lung cancer evolution. *Nature* 2019;567:479-85.
7. Marjanovic ND, Hofree M, Chan JE, et al. Emergence of a High-Plasticity Cell State during Lung Cancer Evolution. *Cancer Cell* 2020;38:229-246.e13.
8. Kerr KM, Bibeau F, Thunnissen E, et al. The evolving landscape of biomarker testing for non-small cell lung cancer in Europe. *Lung Cancer* 2021;154:161-75.
9. Wankhede D, Grover S, Hofman P. Circulating Tumor Cells as a Predictive Biomarker in Resectable Lung Cancer: A Systematic Review and Meta-Analysis. *Cancers (Basel)* 2022;14:6112.
10. Chang S, Shim HS, Kim TJ, et al. Molecular biomarker testing for non-small cell lung cancer: consensus statement of the Korean Cardiopulmonary Pathology Study Group. *J Pathol Transl Med* 2021;55:181-91.
11. Tang H, Wang S, Xiao G, et al. Comprehensive evaluation of published gene expression prognostic signatures for biomarker-based lung cancer clinical studies. *Ann Oncol* 2017;28:733-40.
12. Abbosh C, Birkbak NJ, Wilson GA, et al. Phylogenetic ctDNA analysis depicts early-stage lung cancer evolution. *Nature* 2017;545:446-51.
13. Jamal-Hanjani M, Wilson GA, McGranahan N, et al. Tracking the Evolution of Non-Small-Cell Lung Cancer. *N Engl J Med* 2017;376:2109-21.
14. Ballaz S, Mulshine JL. The potential contributions of chronic inflammation to lung carcinogenesis. *Clin Lung Cancer* 2003;5:46-62.
15. Yoshida C, Kadota K, Yamada K, et al. Tumor-associated CD163(+) macrophage as a predictor of tumor spread through air spaces and with CD25(+) lymphocyte as a prognostic factor in resected stage I lung adenocarcinoma. *Lung Cancer* 2022;167:34-40.
16. Donnem T, Hald SM, Paulsen EE, et al. Stromal CD8+ T-cell Density—A Promising Supplement to TNM Staging in Non-Small Cell Lung Cancer. *Clin Cancer Res* 2015;21:2635-43.
17. Dejima H, Hu X, Chen R, et al. Immune evolution from preneoplasia to invasive lung adenocarcinomas and underlying molecular features. *Nat Commun* 2021;12:2722.
18. Zhang C, Zhang J, Xu FP, et al. Genomic Landscape and Immune Microenvironment Features of Preinvasive and Early Invasive Lung Adenocarcinoma. *J Thorac Oncol* 2019;14:1912-23.
19. Wang Z, Li Z, Zhou K, et al. Deciphering cell lineage specification of human lung adenocarcinoma with single-cell RNA sequencing. *Nat Commun* 2021;12:6500.
20. Zhu J, Fan Y, Xiong Y, et al. Delineating the dynamic evolution from preneoplasia to invasive lung adenocarcinoma by integrating single-cell RNA sequencing and spatial transcriptomics. *Exp Mol Med* 2022;54:2060-76.
21. Shang J, Jiang H, Zhao Y, et al. Differences of molecular events driving pathological and radiological progression of lung adenocarcinoma. *EBioMedicine* 2023;94:104728.
22. Travis WD, Brambilla E, Nicholson AG, et al. The 2015 World Health Organization Classification of Lung Tumors: Impact of Genetic, Clinical and Radiologic Advances Since the 2004 Classification. *J Thorac Oncol* 2015;10:1243-60.
23. Zhang W, Gong C, Peng X, et al. Serum Concentration of CD137 and Tumor Infiltration by M1 Macrophages Predict the Response to Sintilimab plus Bevacizumab Biosimilar in Advanced Hepatocellular Carcinoma Patients. *Clin Cancer Res* 2022;28:3499-508.
24. Cao G, Hua D, Li J, et al. Tumor immune microenvironment changes are associated with response to neoadjuvant chemotherapy and long-term survival benefits in advanced epithelial ovarian cancer: A pilot study. *Front Immunol* 2023;14:1022942.
25. Wang S, Shi H, Liu T, et al. Mutation profile and its correlation with clinicopathology in Chinese hepatocellular carcinoma patients. *Hepatobiliary Surg Nutr* 2021;10:172-9.
26. Bi J, Tian Z. NK Cell Dysfunction and Checkpoint Immunotherapy. *Front Immunol* 2019;10:1999.
27. Park MD, Reyes-Torres I, LeBerichel J, et al. TREM2 macrophages drive NK cell paucity and dysfunction in lung cancer. *Nat Immunol* 2023;24:792-801.
28. Richards JO, Chang X, Blaser BW, et al. Tumor growth impedes natural-killer-cell maturation in the bone marrow. *Blood* 2006;108:246-52.
29. Salcher S, Sturm G, Horvath L, et al. High-resolution

- single-cell atlas reveals diversity and plasticity of tissue-resident neutrophils in non-small cell lung cancer. *Cancer Cell* 2022;40:1503-1520.e8.
30. Zheng X, Weigert A, Reu S, et al. Spatial Density and Distribution of Tumor-Associated Macrophages Predict Survival in Non-Small Cell Lung Carcinoma. *Cancer Res* 2020;80:4414-25.
 31. Aras S, Zaidi MR. TAMEless traitors: macrophages in cancer progression and metastasis. *Br J Cancer* 2017;117:1583-91.
 32. Liu L, Wang C, Li S, et al. Tumor immune microenvironment in epidermal growth factor receptor-mutated non-small cell lung cancer before and after epidermal growth factor receptor tyrosine kinase inhibitor treatment: a narrative review. *Transl Lung Cancer Res* 2021;10:3823-39.
 33. Busch SE, Hanke ML, Kargl J, et al. Lung Cancer Subtypes Generate Unique Immune Responses. *J Immunol* 2016;197:4493-503.
 34. Brusselle GG, Demoor T, Bracke KR, et al. Lymphoid follicles in (very) severe COPD: beneficial or harmful? *Eur Respir J* 2009;34:219-30.
 35. Dieu-Nosjean MC, Goc J, Giraldo NA, et al. Tertiary lymphoid structures in cancer and beyond. *Trends Immunol* 2014;35:571-80.
 36. Germain C, Devi-Marulkar P, Knockaert S, et al. Tertiary Lymphoid Structure-B Cells Narrow Regulatory T Cells Impact in Lung Cancer Patients. *Front Immunol* 2021;12:626776.
 37. Xu X, Gao Y, Duan S, et al. Clinical implications and molecular features of tertiary lymphoid structures in stage I lung adenocarcinoma. *Cancer Med* 2023;12:9547-58.
 38. Giatromanolaki A, Chatzipantelis P, Contrafouris CA, et al. Tertiary Lymphoid Structures, Immune Response, and Prognostic Relevance in Non-Small Cell Lung Cancer. *Cancer Invest* 2023;41:48-57.
 39. Wakasu S, Tagawa T, Haratake N, et al. Preventive effect of tertiary lymphoid structures on lymph node metastasis of lung adenocarcinoma. *Cancer Immunol Immunother* 2023;72:1823-34.
 40. Forde PM, Spicer J, Lu S, et al. Neoadjuvant Nivolumab plus Chemotherapy in Resectable Lung Cancer. *N Engl J Med* 2022;386:1973-85.
 41. Wislez M, Mazieres J, Lavole A, et al. Neoadjuvant durvalumab for resectable non-small-cell lung cancer (NSCLC): results from a multicenter study (IFCT-1601 IONESCO). *J Immunother Cancer* 2022;10:e005636.
 42. Gao S, Li N, Gao S, et al. Neoadjuvant PD-1 inhibitor (Sintilimab) in NSCLC. *J Thorac Oncol* 2020;15:816-26.

Cite this article as: Zhao J, Lu Y, Wang Z, Wang H, Zhang D, Cai J, Zhang B, Zhang J, Huang M, Pircher A, Patel KH, Ke H, Song Y. Tumor immune microenvironment analysis of non-small cell lung cancer development through multiplex immunofluorescence. *Transl Lung Cancer Res* 2024;13(9):2395-2410. doi: 10.21037/tlcr-24-379